C1

CERN PPE 94-19
SW 3408

EUROPEAN ORGANIZATION FOR NUCLEAR RESEARCH

DD

CERN LIBRARIES, GENEVA
P00021941

CERN-PPE/94-19
INFN-AE/94/04
2 February 1994

Construction and test of calorimeter modules for the CHORUS experiment

S. Buontempo[b)], A. Capone[c)], A. G. Cocco[b)], D. De Pedis[c)], E. Di Capua[a)], U. Dore[c)], A. Ereditato[b)*], M. Ferroni[a)], G. Fiorillo[b)], P. F. Loverre[c)], C. Luppi[a)], D. Macina[c)], F. Marchetti-Stasi[b)], M. A. Mazzoni[c)], P. Migliozzi[b)], V. Palladino[b)], G. Piredda[c)], F. Riccardi[b)], S. Ricciardi[a)], P. Righini[c)], B. Saitta[a)], R. Santacesaria[c)], P. Strolin[b)] and P. Zucchelli[a)]

a) *Università and Sezione INFN, Ferrara, Italy*
b) *Università "Federico II" and Sezione INFN, Napoli, Italy*
c) *Università "La Sapienza" and Sezione INFN, Roma, Italy*
* *Also CERN*

(Submitted to Nucl. Instr. & Meth.)

Abstract

The construction of modules and the assembly of the calorimeter for CHORUS, an experiment that searches for $\nu_\mu \longleftrightarrow \nu_\tau$ oscillation, have been completed. Within the experiment, the calorimeter is required to measure the energy of hadronic showers produced in neutrino interactions with a resolution of $\sim \frac{30\%}{\sqrt{E(GeV)}}$. To achieve this performance, the technique, developped in recent years, of embedding scintillating fibers of 1 mm diameter into a lead matrix has been adopted for the most upstream part of the calorimeter. A more conventional system, of alternating layers of lead and scintillator strips, was used for the rest. Details of module construction as well as results obtained when modules were exposed to electron and muon beams are presented.

1. Introduction

The calorimetric technique of embedding scintillating fibers into a lead matrix has been developed in the past years by the LAA-SPACAL Collaborations [1] for applications at future high energy hadron colliders.

It has been found [1, 2] that fibers of $1\,mm$ diameter and a volume ratio of 4:1, with lead as passive and scintillator as active materials assure both compensation and good sampling, resulting in an energy resolution of $\sim 13\%/\sqrt{E(GeV)}$ and of $\sim 30\%/\sqrt{E(GeV)}$ for electromagnetic and hadronic showers respectively.

The calorimeter described in this paper is the first large scale application of such a technique. However, this calorimeter differs from those studied so far for the fibers are placed in a direction transverse to the beam direction, a configuration seldom used up to now. This is required by the function that the calorimeter has to perform within the experiment and constitutes a novelty of the device.

This paper is organized as follows. The conceptual design of the complete calorimeter is presented in Section 2. Details of the construction of the three types of modules which are used are given in Section 3. Section 4 contains a description of the experimental setup where some of these modules were exposed to charged particle beams. In Section 5 the first results on the performance of the individual modules are discussed and conclusions are drawn in Section 6.

2. Design of the calorimeter

The CHORUS experiment [3] searches for $\nu_\mu \longleftrightarrow \nu_\tau$ oscillations in the CERN SPS wide band neutrino beam.

Possible charged current ν_τ interactions, with the subsequent decay of the τ lepton into a muon or pions, are searched for in a target of about $0.8\,t$ of nuclear emulsions, which is followed by the electronic components of the detector (scintillating fiber trackers, an air-core magnet, the calorimeter described in this paper and a muon spectrometer). τ decay candidates have to be isolated from a large background of ordinary ν_μ interactions and it is essential to reduce as much as possible, by means of electronic detectors, the number of events to scan in the nuclear emulsions. This reduction can be achieved by means of a selection on kinematic variables, since the presence of a neutrino in the decay results in an unbalance of the visible transverse momentum. Such a selection is more effective if the hadronic shower produced in the interaction is measured with high energy and angular resolution.

It is also important to have the capability to track through-going muons and to match their trajectories with those determined in the other detectors of the apparatus, a requirement that has not played an important role in the applications, considered so far, of calorimeters of this type at colliders. Therefore the calorimeter must be a *tracking device*, with the fibers placed in a direction perpendicular to that of the incident particles and longitudinal segmentation is also necessary to allow for the insertion of limited streamer tube chambers. Furthermore, the size of the

neutrino beam requires modules of considerable length. This makes the problems generated by the attenuation of the light - that has to travel through considerable distances to reach the photomultipliers - potentially more serious than in other calorimeters based upon the same principle, but with a longitudinal orientation of the fibers.

The calorimeter designed for the CHORUS experiment satisfies the requirements mentioned above and overcomes satisfactorily these difficulties. Results of earlier tests on prototype modules that helped to finalize the design, have already been reported [4].

It has a modular construction, in which the elements are arranged to form planes which are oriented normally to the beam, alternately in the horizontal and vertical directions. To reconstruct the center of gravity of the energy deposited by the hadrons emitted in the interactions with good accuracy, the width of the modules was chosen to be much smaller than the size of the average hadron shower.

The calorimeter consists of three sectors with decreasing granularity, called EM, HAD1 and HAD2. The first sector will measure the electromagnetic component of the hadronic shower in the neutrino induced events, while the other two sectors will complete the measurement of the hadronic component. The total depth is about 5.2 interaction lengths, sufficient to contain 99% of the shower produced by a pion of $5\,GeV/c$ momentum. It should be observed that $\sim$ 90% of the hadrons produced in the neutrino interactions have momentum less than $5\,GeV$.

The first two sectors of the calorimeter are made of scintillating fibers and lead, the third sector is made as a sandwich of lead and scintillating strips. The structure of the calorimeter allows light collection through photomultipliers on both sides of the module and this is exploited to reduce effects of light attenuation.

Between the horizontal and the vertical planes of calorimeter modules, limited streamer tube planes are inserted to allow tracking of penetrating charged particles and are arranged in pairs (to have two coordinates). The streamer tubes were previously used for the CHARM II experiment and their characteristics and performances are described in [5]. In CHORUS, however, only the digital signals from the wires are recorded.

The main features of the calorimeter are summarized in Table 1 and its isometric view is shown in Fig.1. It is mounted on a support standing on rails, so that it can be moved off the detector axis to perform dedicated energy calibration with electron and pion beams.

3. Module construction

A careful check on the quality of the scintillating materials was performed. All the 900 scintillator strips and a sample, corresponding to 4% of the fibers, were tested, to verify that individual attenuation length and light output were adequate for our purposes. For the fiber tests, a special device was built at INFN Naples [6], while more conventional means (β-source and multi channel analyser) were used for

	EM	HAD1	HAD2	Total
Module Dimension (mm)	40 × 80 × 2620	80 × 80 × 3350	100 × 200 × 3690	—
Number of Planes	4	5	5	14
Depth: $X_0(\lambda_{int})$	21.5 (0.78)	55.2 (2.0)	67.1 (2.44)	143.8 (5.22)
Number of Modules	124	200	90	414
PM Type	Hamamatsu R1355/SM	Thorn - EMI 9839A	Thorn - EMI 9839A	—
PM per Module	4	2	4	—
Total Number of PM	496	400	360	1256
Fibers/Strips Type	Kuraray SCS-F81	Bicron BCF-12	Bicron BC-408 (strips)	—
Number of fibers/strips	93000	310800	900	404700
Total Length (km)	283	1165	3	1451
Pb Weight (tons)	9.7	42	60	111.7
Scintillator Weight (tons)	0.22	0.92	1.32	2.46

Table 1: Characteristics of the calorimeter.

the strips.

3.1 Electromagnetic modules

The electromagnetic sector is composed of two horizontal and two vertical planes of 31 modules each. These are built by piling up extruded layers of grooved lead and plastic scintillating fibers positioned in the grooves. A module consists of a pile of 21 layers, 2620 mm long and 82.4 mm wide, and 740 fibers of 1 mm diameter and 3050 mm long. On both sides, fibers are arranged in two groups, defining two different read-out cells with about 40 × 40 mm cross-section each (Fig. 2). Each of the four groups is coupled via a plexiglas light guide to a 1" photomultiplier. The pile is kept together by a steel box.

The cross-section of the basic lead layer [1] is shown in Fig. 3. The groove diameter is 1.1 mm and the sheet thickness 1.9 mm. The layer material is 99% lead with 1% antimony content, which improves its mechanical properties. An overall

[1] The lead layers were manufactured by Centro Servizi Metalli, Milano.

thickness disuniformity of less than 2% was achieved through the extrusion procedure.

The fibers were manufactured by Kuraray and are of the type SCSF81. They consist of a polystyrene core surrounded by a $30\,\mu m$ thick acrylic cladding, and emit in the blue, with a maximum around $420\,nm$. A reduction in the light attenuation is obtained by painting the surface of the last 5 centimeters of the fibers (on each side) by acrylic black paint. This has the effect of reducing the light from the cladding, which has a smaller attenuation length. About 93000 fibers were used to build the electromagnetic modules, for a total length of $280\,Km$.

The construction is performed by alternating on a L-shaped steel half-box ($0.8mm$ thick) lead and fiber layers. After the last (lead) layer the second half-box is positioned. A double-sided special adhesive paper is glued between the lateral internal face of the second half-box and the edge of the lead sheet pile. The box is finally closed by soldering the two halves, kept together by applying an appropriate pressure. The adhesive paper is needed to prevent sliding of the layers in the vertical modules; in addition, a ridge mechanically blocks the layers.

Once the box is closed, fibers are grouped at both ends into two sets - so as to form the two read-out cells - and the faces of the bundles are finally milled and polished. The cross-section of the fiber bundles is hexagonal ($22.2\,mm$ apex to apex) and they are coupled to a plexiglas light guide, also with hexagonal cross-section ($24\,mm$ apex to apex). The hexagonal shape and the length of the light guide have been chosen to reduce disuniformities in the mixing of the light coming out of the individual fibers [1]. The light guides are then coupled to 1" photomultipliers, type R1355/SM from Hamamatsu, with a special green extended photocathode, of $24\,mm$ useful diameter. The window of the photomultiplier is covered by a yellow filter Kodak Wratten n.3, which absorbs light with wavelength less than $450\,nm$ and therefore selects the spectral component which has larger attenuation length. Two aluminum boxes (one at each side) house pairs of light guides, photomultipliers, voltage dividers, and mumetals. The boxes are light tight and are closed by PVC plates holding the high voltage and signal connectors.

The EM modules were constructed in the laboratories of INFN Naples.

3.2 HAD1 modules

Each of the five planes of the HAD1 part of the calorimeter is formed by 40 modules, each made of 43 extruded layers of lead identical in height and groove size to those used for the EM sector, but with a length of $3350\,mm$. (see Fig. 4). The grooves accomodate scintillating fibers (Bicron BCF-12) of $1\,mm$ diameter and $3810\,mm$ length, for a total of 1554 fibers per module and a total length of $\sim 1200\,km$. The performance of this type of fibers is comparable with that used for the electromagnetic part of the calorimeter. The lead layers are encased in a stainless steel box ($1\,mm$ thick) to ensure mechanical stability.

Fibers are collected at both ends in an hexagonal bundle whose polished

end is coupled, via a light pipe, to a 2" photomultiplier (EMI 9839 A), previously used in the CHARM II experiment. The empty space of the boxes around the fiber bundles is filled with an epoxidic resin (Araldit D) with microballons of a phenolic resin as an additive, to avoid sliding of the lead sheets in vertical modules. This mixture contains also a small percentage of carbon black to reduce light leaks and the contribution of light from the cladding, playing therefore the same role as that of the black paint in the EM type modules.

The modules were assembled by Pol.Hi.Tech. at Carsoli (Italy), using a semiauthomatic device developed by INFN Rome. The steps followed at assembly stage are similar to those employed for the construction of electromagnetic modules; the steel box, in this case, is compressed with a total force of $9 \times 10^4 N$. The fibers are collected together and are extracted from the terminal parts of the boxes. At this stage the filling mixture, whose hardening time is about 24 hours, is poured in. The faces of the bundles are then milled and polished and a first test of optical quality of the whole assembly is made. For mechanical reasons, the lead sheets of EM and HAD1 modules have a different orientation relative to the beam direction, as illustrated in Fig. 2 and 4.

3.3 HAD2 modules

The HAD2 sector is made of five planes (three vertical and two horizontal) of 18 modules each, for a total of 90 modules and a mass of about $60\,t$.

Each module is constructed by superposing five alternate layers of one lead bar made of 99% lead and 1% antimony ($3690 \times 200 \times 16$ *mm*) and two adjacent scintillator strips (BICRON, BC-408) $3714 \times 100 \times 4$ *mm* packed in a 0.5 *mm* thick stainless steel box open at both ends (see Fig. 5), made of two halves held together by rivets.

Within one module, each of the two groups of five scintillator strips is coupled to 2" photomultipliers - of the same type used for HAD1 - at both ends via plexiglas light guides; therefore a single module is seen by a total of four photomultiplier tubes, and thus contains two read-out cells. Details of the optical coupling of the scintillator to the photomultiplier are shown in Fig. 6. Five trapezoidal, laser-cut, plexiglas plates, $6mm$ thick, $200mm$ long and $100mm$ and $40mm$ bases, are glued to the scintillator strips prior to their insertion in the calorimeter modules, using an optical cement (BC-600) with an index of refraction close to that of the scintillator. A groove of $4mm$ width and $2mm$ depth forming an angle with the vertical plane - varying according to the position of the light guide in the vertical stack (see Fig. 6) - was machined at the wider end to ensure a good contact with the scintillator.

A special device was constructed to allow the simultaneous glueing of two sets of five scintillator strips with the possibility of applying pressure individually on each of the plexiglas plates at glueing stage; the hardening time was 24 hours. Once assembled in the steel box with the lead bars, the ends of the plexiglas plates were milled directly on the assembly table and glued, with a plexiglas epoxy (Acrifix 106, by Roehm) to a light guide of the shape shown in Fig. 6. The scintillator strips were supplied with a light tight wrapping about $0.5\,mm$ thick, reflective on the inside; the

plexiglas guides were made light tight by using a foil of black plastic material with an aluminised inner coating, provided by Prodicon.

The attenuation length and light yield of each scintillator strip were measured, before glueing, using a radioactive source; it was found that the distributions had a spread about their mean value of 13% and 5%, respectively.

Because of their weight, the HAD2 modules were assembled at CERN, close the site of the CHORUS apparatus.

4. Test beam setup

While a check on the quality of nearly all the modules was performed using cosmic rays, some were exposed to a charged particle beam to gather detailed information on their expected performance and resolution.

A testing station was prepared in the X7B area of the X7 test beam at CERN, and data were taken in November 1992 and May 1993 with electrons, positrons and muons, the test with pions being meaningful only with the assembled calorimeter, which provides an adequate number of interaction lengths.

The setup is shown in Fig. 7. Coincidences between the scintillation counters $T_1 \cdot T_2 \cdot \bar{H}$ (and when required $T_3 \cdot T_4$) constituted the main trigger. The data acquisition was based on a FIC 8232 system (running SPIDER under OS9) and communicating with CAMAC through a VIC bus [7]. Real time monitoring and analysis were possible on a DEC Vax Station connected to the acquisition setup through ethernet. The analog signal from the photomultipliers was digitised by a dual-range 8-bit ADC to increase the dynamic range, with the conversion ratio chosen according to the type of module, in a fashion similar to that adopted in the CHARM experiment [8].

The modules to be tested were placed on a support that could move in the two directions perpendicular to the beam line of flight, thus allowing to study possible dependence of the performance on the position of the impact point of the beam on the module. This impact point was defined with an accuracy of $\sim 1\,cm$ and angular resolution of $\sim 1\,mrad$, with the help of the counters F_1 and F_2, made out of four smaller scintillators of $1\,cm \times 1\,cm \times 8\,cm$ each.

Data were taken at electron momenta varying between 2.5 and $10\,GeV/c$ and with $100\,GeV/c$ muons. Different types of modules were tested individually and, to achieve good containment for electromagnetic showers, six modules of the EM and six of HAD1 types were packed together to form two *walls*, as shown in the insert of Fig. 7 with a depth of comparable number of radiation lengths ($\sim 17\,X_0$ for EM, $\sim 22\,X_0$ for HAD1). A similar arrangement was not necessary for the HAD2 type since a single module corresponds to $\sim 15\,X_0$. In this paper, these three configurations will be referred to as W1,W2,W3. In addition, one of the HAD2 modules was placed

beyond the movable support to provide a measurement of longitudinal leakage.

5. Analysis and results

5.1 Light attenuation lengths and longitudinal uniformity

A typical response to $100\,GeV/c$ negative muons incident at the centre of each of the three types of modules is shown in Fig. 8. Voltage on the photomultipliers was set so that minimum ionising particles would give a signal whose most probable value, when digitised, corresponded to a channel between 25 and 50 of the high sensitivity part of the dual-range ADC. Fig. 9 shows the response of the detectors in the W1, W2 and W3 configurations to electrons of $3\,GeV/c$ nominal momentum, where losses due to longitudinal leakage are expected to be small.

To determine attenuation lengths and to study the longitudinal uniformity of the three types of detectors, a horizontal scan over different impact points of the beam was performed.

For the EM-type modules, the attenuation length was determined using the most probable value of the energy released by $100\,GeV/c$ muons (peak of Landau distribution) as a function of distance from the photomultiplier [2]. The data are shown in Fig. 10a, where the line represents the result of a fit to a single exponential form of the type $e^{-x/\lambda}$ to the points. Averaging over ten modules, a mean value of $462\,cm$ for λ was obtained, with a spread of $53\,cm$ about this mean value. In Fig. 10b the sum of the pulse heights of photomultipliers situated at opposite sides is plotted for various impact points of the beam along the module and it exhibits the expected uniform behaviour, namely a signal which depend only very weakly upon the beam incidence point. A similar behaviour (see Fig. 10c) is also observed with electrons incident on the W1 configuration (EM-wall). In this case the signals from all the photomultipliers connected to all the modules that make up the *wall* are combined. Systematic differences in the response of the detector when particles are incident at the centre or at the edge of the module are very small. The dashed line in Fig. 10c represents the signal averaged over the different impact points. The ratio between the rms spread of the points about this mean value and the average, gives an estimate of the degree of uniformity of the EM-*wall*. For electrons of $3\,GeV/c$ momentum, this ratio was less than 1%.

Fig. 11a shows the results of the analysis of data taken with a $3\,GeV/c$ electron beam hitting the central longitudinal axis of a read-out cell of HAD2 (the part of the calorimeter equipped with scintillator strips), at five different impact points, starting at 25 *cm* distance from the light guide, with and without filters (KODAK Wratten n.3). These studies with yellow filters were required to optimise the performance of the photomultipliers used for the modules of the type HAD1 and HAD2 which

[2] Muons were preferred in this case over electrons, to avoid systematic errors due to the rather wide pulse height distribution observed in a single EM module with incident electrons, originating from the incomplete containment of the shower (only $\sim 30\%$ at $3\,GeV$).

were recycled from the CHARM II experiment. As expected, an increase in the value of the light attenuation length, as well as a less pronounced deviation from a single exponential form are evident, in the data taken with filters. Averaging over the five HAD2 modules tested in the X7 beam (corresponding to ten read-out cells), the mean attenuation length with filters is $362\,cm$ with $50\,cm$ rms spread and $(251 \pm 30)\,cm$ without filters. As it is shown in Fig. 11b, the sum of left and right pulses shows little dependence on the distance of the particle impact point from the photomultiplier ($< 10\%$) while the maximum deviation measured without filters amounts to $\sim 25\%$.

A systematic study of the effect of filters was made only for the HAD2-type modules. However some measurements were repeated using the HAD1 modules and these confirmed the conclusions, as it might have been expected since they are equipped with the same type of photomultipliers and the emission spectra of the fibers and the scintillator strips are similar.

Fig. 12a and 12b show the response of one HAD1-type module to $3\,GeV$ electrons as a function of the distance from the photomultiplier. As expected, they exhibit the same behaviour as the other detectors. When averaged over ten modules, for the attenuation length λ, a value of $220cm$ with a $20cm$ rms spread about this mean value, is obtained without filters. An improvement of $\sim 30\%$ is obtained when filters are used.

Since physical processes are observed by photomultipliers at both ends of the module, it is possible to estimate the number of photoelectrons produced at the cathode using the relation

$$N_{pe} = \frac{2 < N >^2}{\sigma_\Delta^2}$$

where σ_Δ is the standard deviation of the distribution of the difference of left and right ADC counts and $< N >$ is their common average value. This formula is valid in the approximation of complete symmetry left-right in light propagation, collection and photocathode efficiencies. It was found that, without filters for HAD1 and HAD2, when electrons of energy E are incident at the center of the module, the cathode of a single photomultiplier would produce $\sim 170 \cdot E$, $\sim 280 \cdot E$ and $\sim 270 \cdot E$ (with E in GeV) photoelectrons. The use of filters in HAD1 and HAD2 of course reduces the number of photons reaching the photocathode. It was computed that in these conditions the number of photoelectrons per GeV is reduced to ~ 140 and ~ 110 respectively for the two detectors. The effect of this reduction on the amplitude of the signal was partly compensated by increasing the operating voltage of the photomultipliers. This does not constitute a problem however, since the absolute number photoelectrons is adequate and does not deteriorate appreciably the energy resolution (see section 5.2). Furthermore, in these conditions the modules are capable of detecting with full efficiency minimum ionising particles that cross at the far end (about $3.7m$ for HAD2).

This is illustrated in Fig. 13, where the signal obtained with muons at an impact point of $345\,cm$ is shown and compared to that at the center of the module. On the basis of these results, it was decided to adopt filters also for the HAD1 and HAD2 modules.

5.2 Energy response and resolution

The response (mean pulse height) of the detectors, in the configurations W1, W2 and W3, as function of the nominal momentum of electrons, incident at the center of the modules, is shown in Fig. 14. As expected, the measured points lie on a straight line, and the results of a fit of the type $a \cdot E + b$ are shown in Fig. 14, superimposed to the data. They show that, in all cases, extrapolation to zero energy leads to a *positive* value of the pulse height. Both a systematic shift of about $300 MeV/c$ in the nominal beam momentum or a non linear behaviour of the detectors at low energy, could generate such an effect.

Several tests were performed to investigate whether its origin is beam related. These included the use of a lead glass detector to have an independent check on the linearity and the extrapolation, as well as data taking with a positive beam, to invert the polarity of the magnets.

These studies showed, in a conclusive manner, evidence of a systematic shift in the beam momentum. Its actual value depended upon the history of the momentum defining magnet and averaged to approximately $280 MeV/c$ [3]. This average correction will be applied in the determination of the energy resolution.

The energy resolution is shown as a function of energy in Fig. 15, separately for the three detectors. The energy dependence is well described by the parameterisation

$$\frac{\sigma}{E} = \frac{a}{\sqrt{E}} + b$$

(with E in GeV) represented by the lines in Fig. 15. The values of a and b are given in Table 2, for the two cases, usually considered in recent literature, of a linear or quadratic sum of the two terms contributing to the resolution. The resolution for electromagnetic showers measured by the sectors that use fibers, agrees with the results obtained with similar calorimeters [1, 10, 11]. That measured in the sector equipped with scintillator strips, agrees also with predictions of Montecarlo simulations. Thus we are confident that, when measured in the completely assembled calorimeter, the energy resolution for hadronic showers will not differ much from the expected $\frac{30\%}{\sqrt{E(GeV)}}$.

6. Conclusions

We have constructed and tested modules of a $110\,t$ calorimeter, part of which $(50\,t)$ represents the first large scale experimental application of the lead-scintillating

[3] This figure is $\sim 40\%$ larger than the value of $200 MeV/c$ that beam experts consider plausible [9].

	$\frac{a}{\sqrt{E}} + b$		$\frac{a}{\sqrt{E}} \oplus b$	
Type of Module	a	b	a	b
EM	0.139 ± 0.003	0.001 ± 0.001	0.141 ± 0.002	0.007 ± 0.005
HAD1	0.125 ± 0.005	0.005 ± 0.002	0.131 ± 0.003	0.016 ± 0.003
HAD2	0.296 ± 0.005	0.001 ± 0.002	0.297 ± 0.002	0.012 ± 0.009

Table 2: Values of parameters obtained fitting the resolution with the functions described in the text.

fiber technique. Because of the special requirements imposed by the use of this calorimeter in the neutrino oscillation experiment CHORUS, its geometry is transverse to the direction of the incident particles, contrary to the configuration typically envisaged for collider applications. The use of scintillating material (fibers and strips) of excellent quality was paramount to overcome potential difficulties related to this geometry and to the considerable size of the modules. Measured attenuation lengths of more than $3\,m$ and light collection at both ends ensure small corrections and good uniformity. Results from an exposure of the different modules to an electron beam, indicate that the response to electromagnetic showers agrees with the expectations, as far as linearity and energy resolution are concerned. The response of the calorimeter as a whole to electrons and pions will be studied in a forthcoming test, where the *high* resolution of the calorimeter for hadrons, required by the experiment, will be verified.

7. Acknowledgments

The design, construction and installation of this calorimeter in less than one year would have not been possible without the constant support of the technical staff of the collaborating institutions and of CERN. In particular, special thanks are due to Vito Carassiti for the design and supervision of the mechanical aspects of the whole project and to G. Basti, G. Passeggio and R. Gorini for their work on the design. The help of S. Bigoni, G. Bonora, F. Evangelisti, G. Improta, A. Iaciofano, M. Melchiorri, R. Rocco and S. Sabbioni in the design and construction of the large number of tools necessary to make the assembly easier and for the actual assembly of the modules and of the calorimeter itself, is gratefully acknowledged. For the construction of EM modules at INFN Naples, we express our appreciation for the skillfull work of M. Borriello, C. Caiazzo, D. Cocozza, F. Esposito, C. Farella, A. Improta, V. Marzullo, C. Molino, F. Pagano and G. Vanzanella. The mechanical workshop and the drawing office of INFN Rome were essential in the design and construction of the machine for module assembly. Thanks are also due to the

personnel of Pol. Hi. Tech. at Carsoli for the care during the construction and to F. Pulcinella for his work on the electronics necessary for the readout. The efforts of the personnel from the administrative offices made material procurement and border crossing, very smooth. We are indebted to L. Gatignon of CERN for the help, at all hours, during the tests with the X7 beam. This project was made possible by the financial support of INFN.

8. References

1. D. Acosta et al., *Nucl. Instr. and Meth.* **A294** (1990) 193.
2. D. Acosta et al., *Nucl. Instr. and Meth.* **A308** (1991) 481.
3. N. Armenise et al., CHORUS Collaboration, CERN - SPSC/90-42; M. de Jong et al., CHORUS Collaboration, CERN - PPE/93-134.
4. S. Buontempo et al., *Nucl. Phys.* (Proc. Suppl.) **B32** (1993) 70; S. Buontempo et al., presented at the III *International Conference on Calorimetry in High Energy Physics*, Chorpus Christi, USA, 1992.
5. J. P. DeWulf et al., CHARM II Collaboration, *Nucl. Instr. and Meth.* **A252** (1986) 443; *Nucl. Instr. and Meth.* **A263** (1988) 109; *Nucl. Instr. and Meth.* **A278** (1989) 670.
6. S. Buontempo et al., presented at the *5th Topical Seminar on Experimental Apparatus for High Energy Physics and Astrophysics* S. Miniato, Italy, 1993.
7. M.A. Mazzoni and P. Zucchelli, *DAQ System for the calorimeter test*, Internal Note (1992) (unpublished).
8. A.N. Diddens et al., *Nucl. Instr. and Meth.* **178** (1980) 27.
9. L. Gatignon, private communication.
10. G. Anzivino, presented at IV *International Conference on Calorimetry in High Energy Physics*, La Biodola, Isola d'Elba, Italy, 1993.
11. S. Miscetti, for the KLOE Collaboration, presented at IV *International Conference on Calorimetry in High Energy Physics*, La Biodola, Isola d'Elba, Italy, 1993.

Figure Caption

1. Isometric view of the calorimeter.
2. (a) Cross section of EM-type module. The lead sheets are perpendicular to the beam direction, represented by the arrow. (b) Details of grouping of scintillating fibers and optical coupling in EM-type modules. The metal housing for the photomultipliers is also shown.
3. Grooved lead sheet that constitutes the basic building element of EM and HAD1-type modules.
4. Details of HAD1-type modules. Shown are cross section, grouping of fibers (hexagonal bundle) and housing for light guide and photomultiplier. Note that the orientation with respect to the beam direction is different from that of EM-type modules.
5. Cross section of HAD2-type module. Visible are also the screws that hold the lead sheets in the modules placed vertically.
6. Details of the optical coupling for the HAD2-type modules.
7. Experimental setup used during the test of some of the modules in the X7B beam at CERN.
8. Response of the three types of modules to muons of $100\,GeV/c$ momentum. (a) EM; (b) HAD1; (c) HAD2.
9. Response of the three types of detectors to electrons of $3\,GeV/c$ nominal momentum. (a) EM; (b) HAD1; (c) HAD2.
10. Performance of EM-type modules. (a) Response to $100\,GeV/c$ muons as a function of the distance from the photomultiplier. The dashed line represents the result of a fit of the type $A \cdot e^{-x/\lambda}$; for this particular module an attenuation length of $\lambda = 455\,cm$ was obtained. (b) Sum of the signals from the left and right photomultipliers for different points of incidence of the muon beam along the module. The center of the module is at zero on the horizontal axis. (c) Sum of all signals (left and right photomultipliers) recorded by the six modules in the W1 configuration (see text) for $3\,GeV/c$ incident electrons, for different impact points of the beam. The center of the module is at zero on the horizontal axis. Note the very small difference between the signal observed with the beam is incident at the center (zero) or at the edge. The dashed line represents the value of the signal when averaged over the different impact points. A measure of the non-uniformity along the module may be given by the dispersion of the individual measurements about the mean value. The rms spread divided by the mean value is 0.008.

11. Performance of HAD2-type modules. (a) Signal for $3\,GeV/c$ electrons as a function of the distance from the photomultiplier with and without the use of yellow filters. The lines are the results of fits of the type $A \cdot e^{-x/\lambda}$. (b) Sum of the signal seen by photomultipliers at both ends as a function of the beam impact point. The lines represent the expected behaviour if the signals collected were attenuated following an exponential law.

12. As Fig. 11 but for HAD1-type modules.

13. Response of HAD2-type modules to muons incident near the edge (a) and at the center (b) of the module (these correspond to a distance of 345 and of $185\,cm$ from the photomultiplier, respectively).

14. Mean pulse height for the three detectors as a function of nominal momentum of electrons incident at the center of the module. (a) W1; (b) W2; (c) W3. The lines are the results of a linear fit.

15. Resolution of the three detectors as a function of the energy of the incident electron. EM:squares; HAD1:triangles; HAD2:circles. The beam impact point is the center of the module. The lines are results of the fit described in the text.

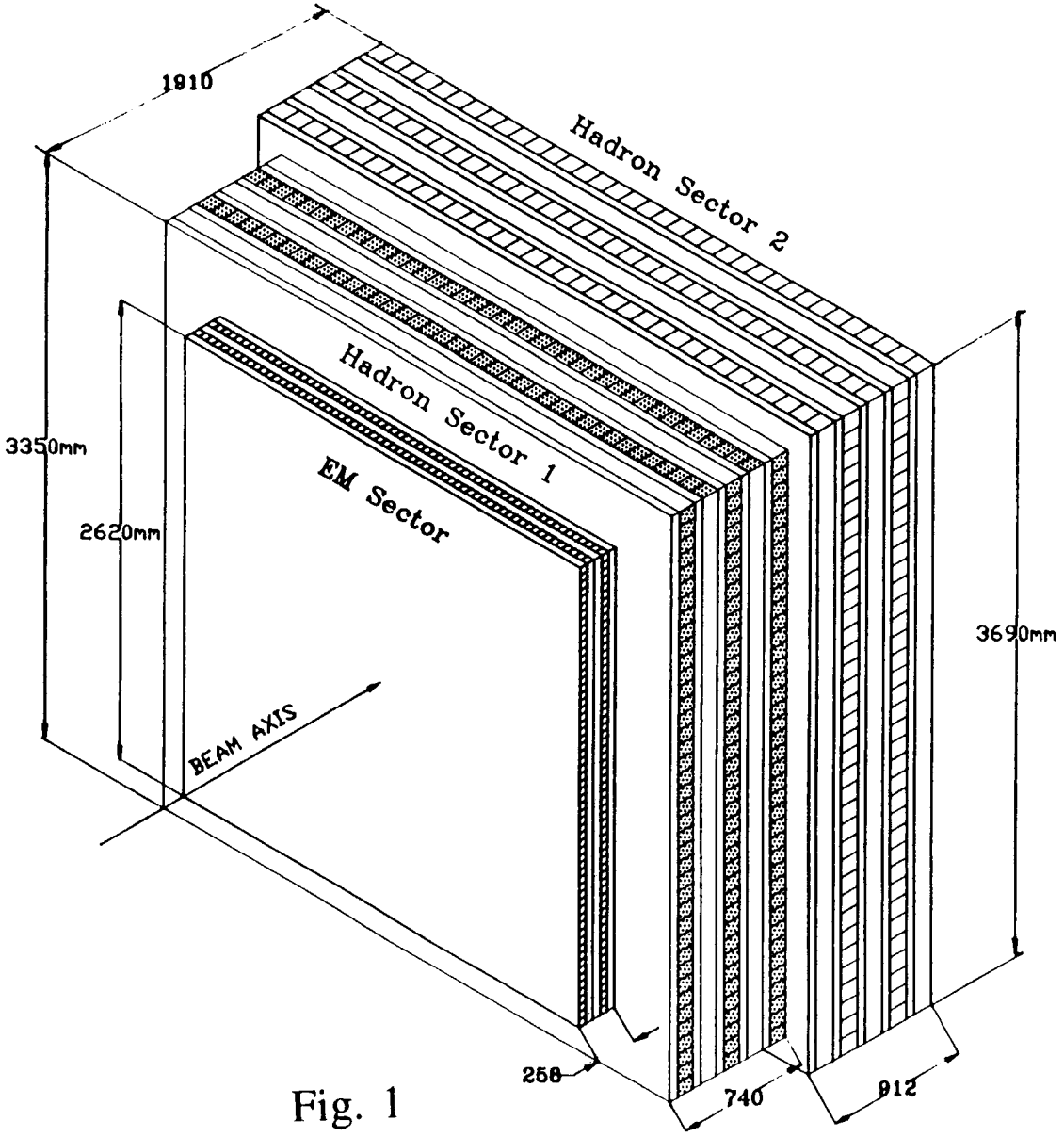
1910
Hadron Sector 2
Hadron Sector 1
EM Sector
3350mm
2620mm
3690mm
BEAM AXIS
258
740
912

Fig. 1

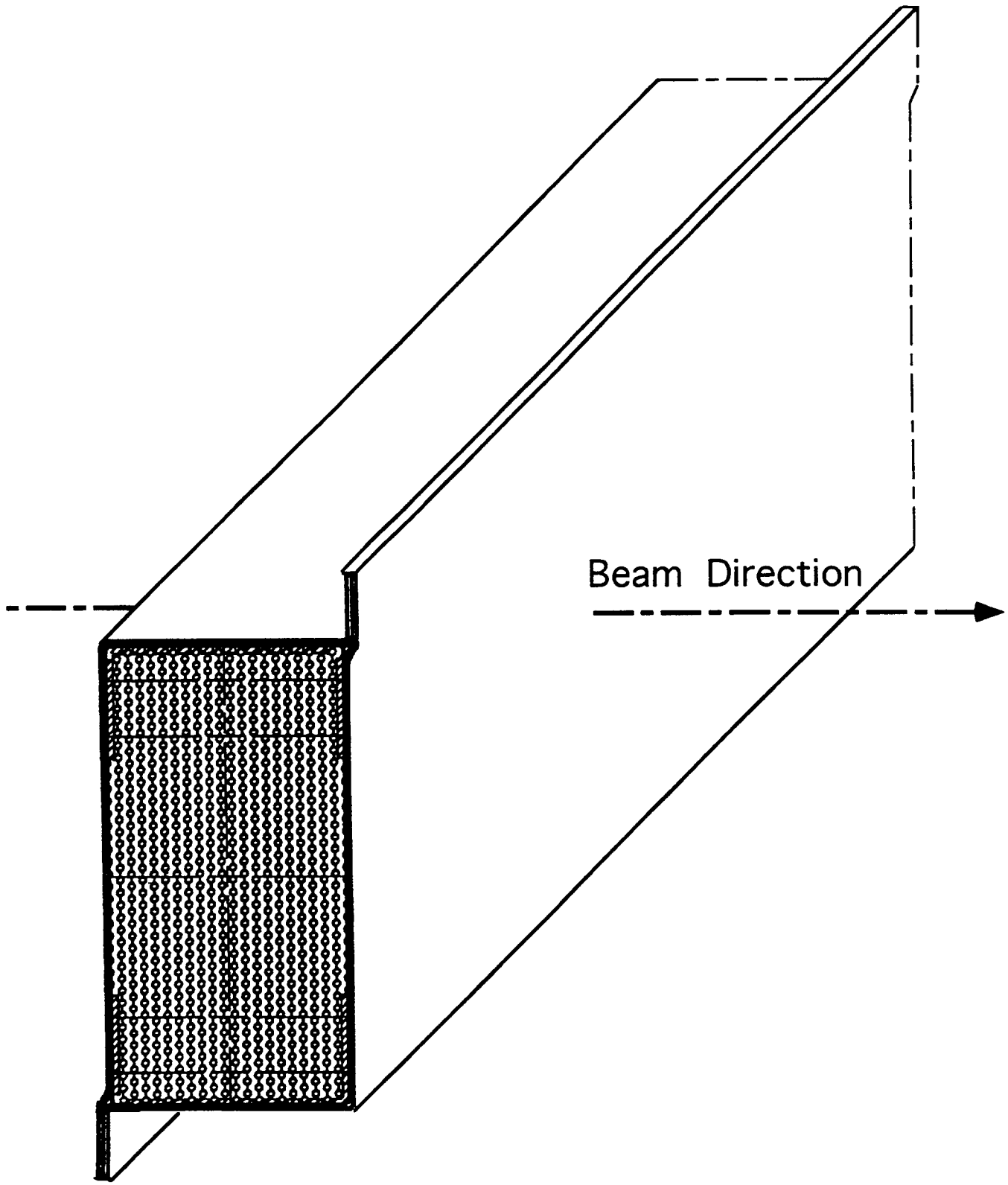

Fig. 2(a)

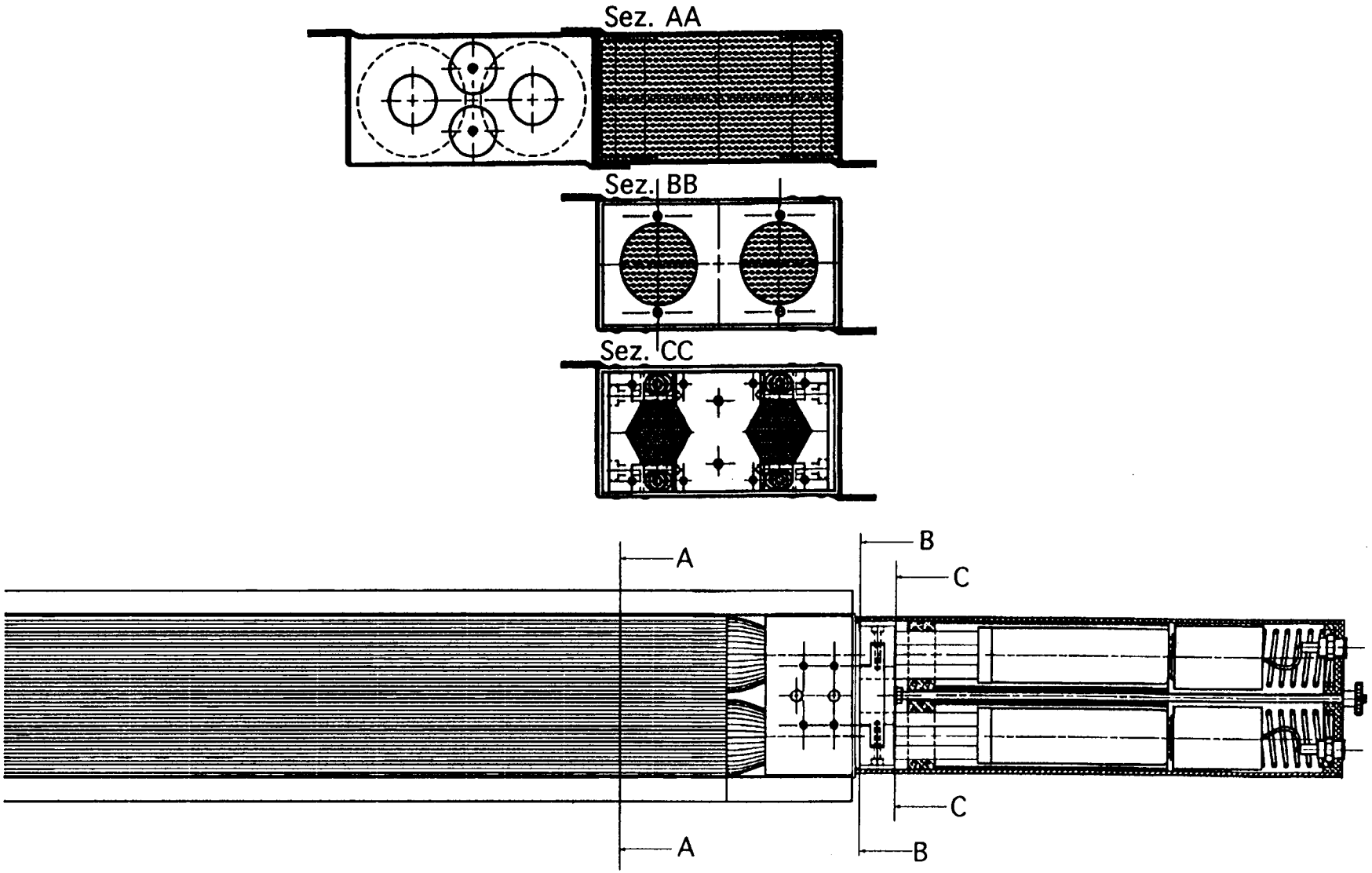

Fig. 2(b)

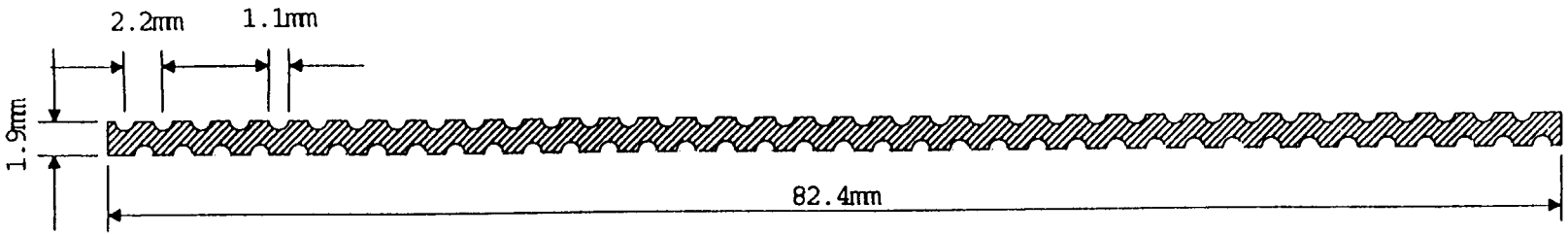

Fig. 3

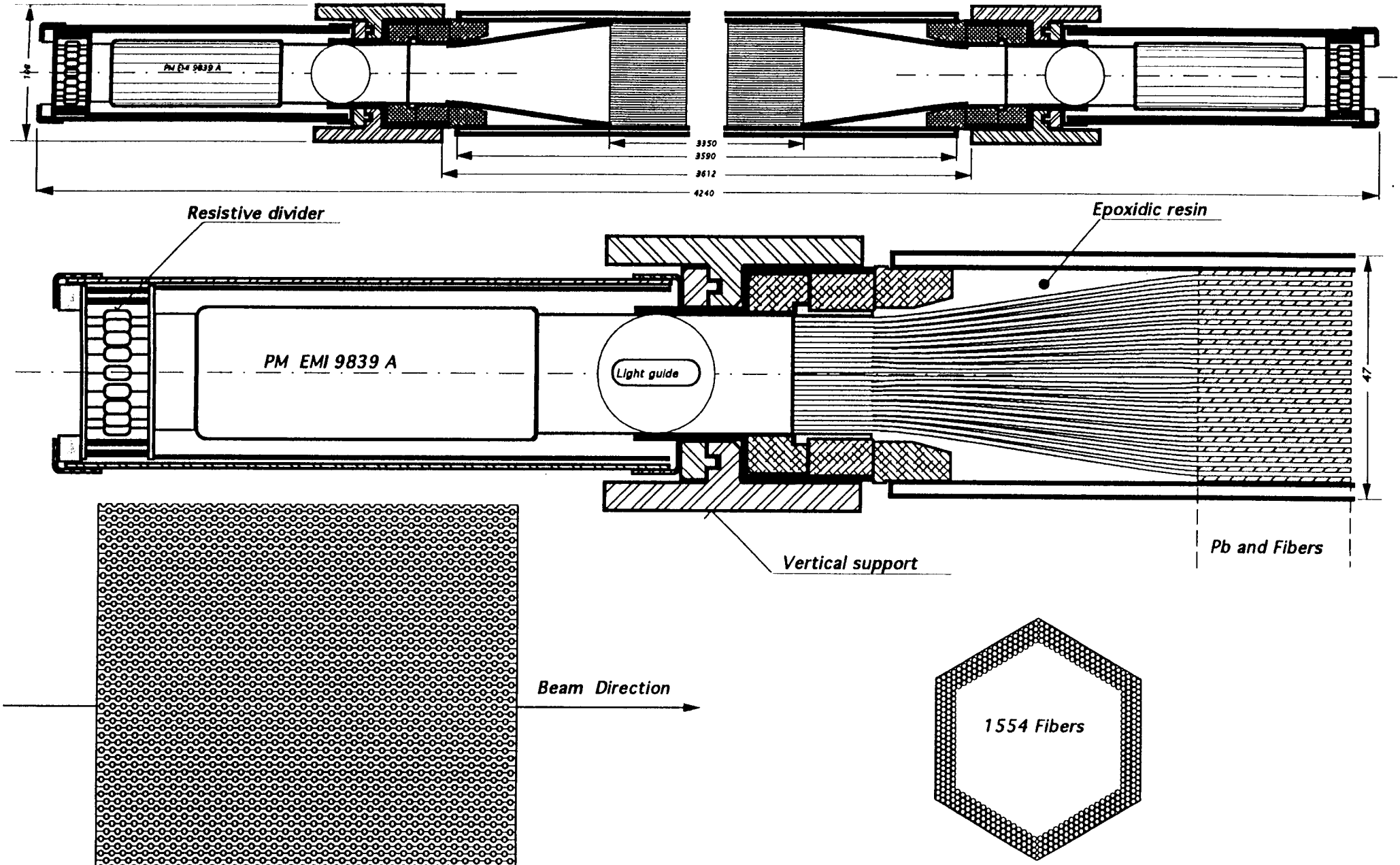
PM EMI 9839 A
3350
3590
3612
4240
Resistive divider
Epoxidic resin
PM EMI 9839 A
Light guide
47
Vertical support
Pb and Fibers
Beam Direction
1554 Fibers
Pb Cross Section

Fig. 4

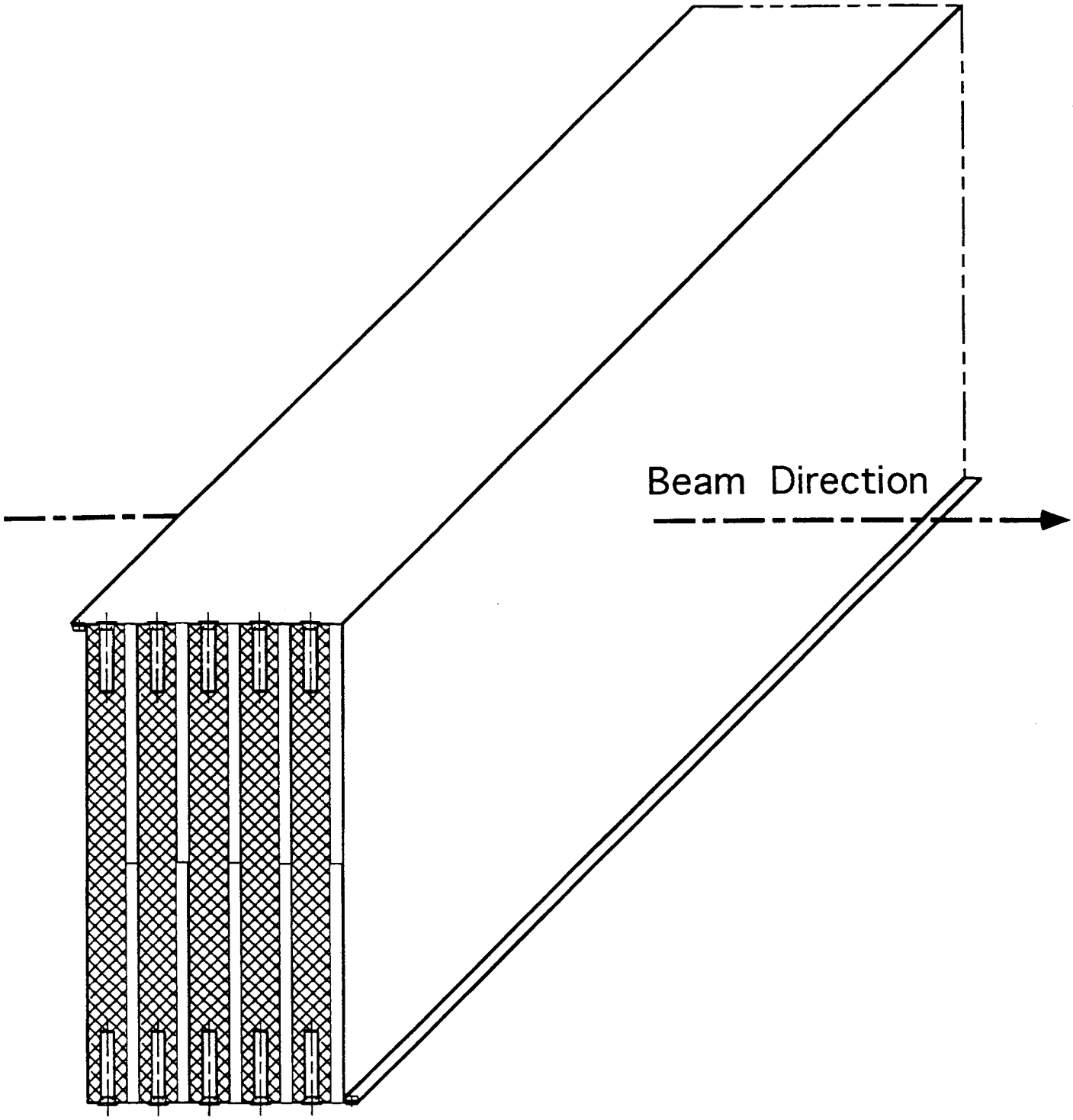

Fig. 5

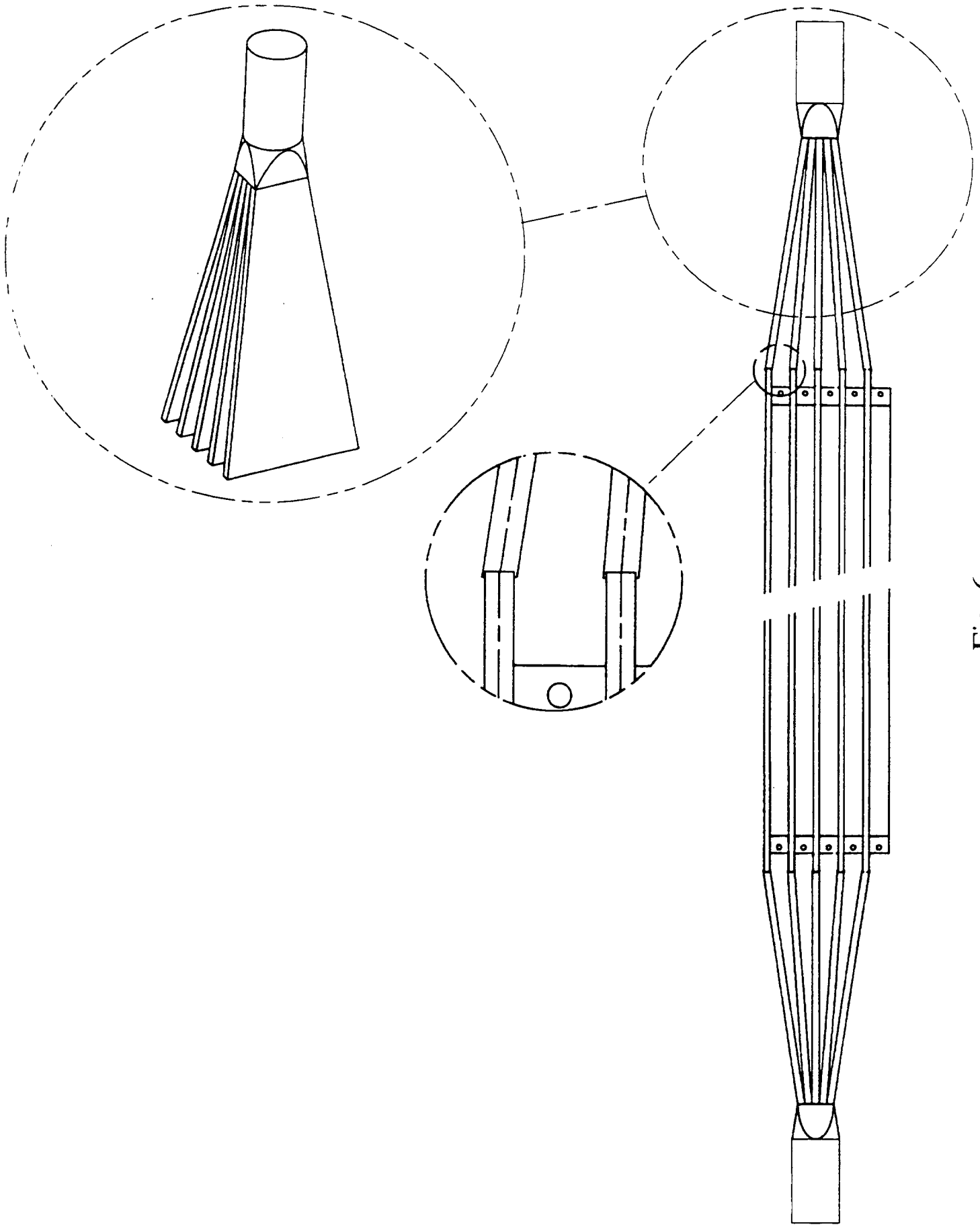

Fig. 6

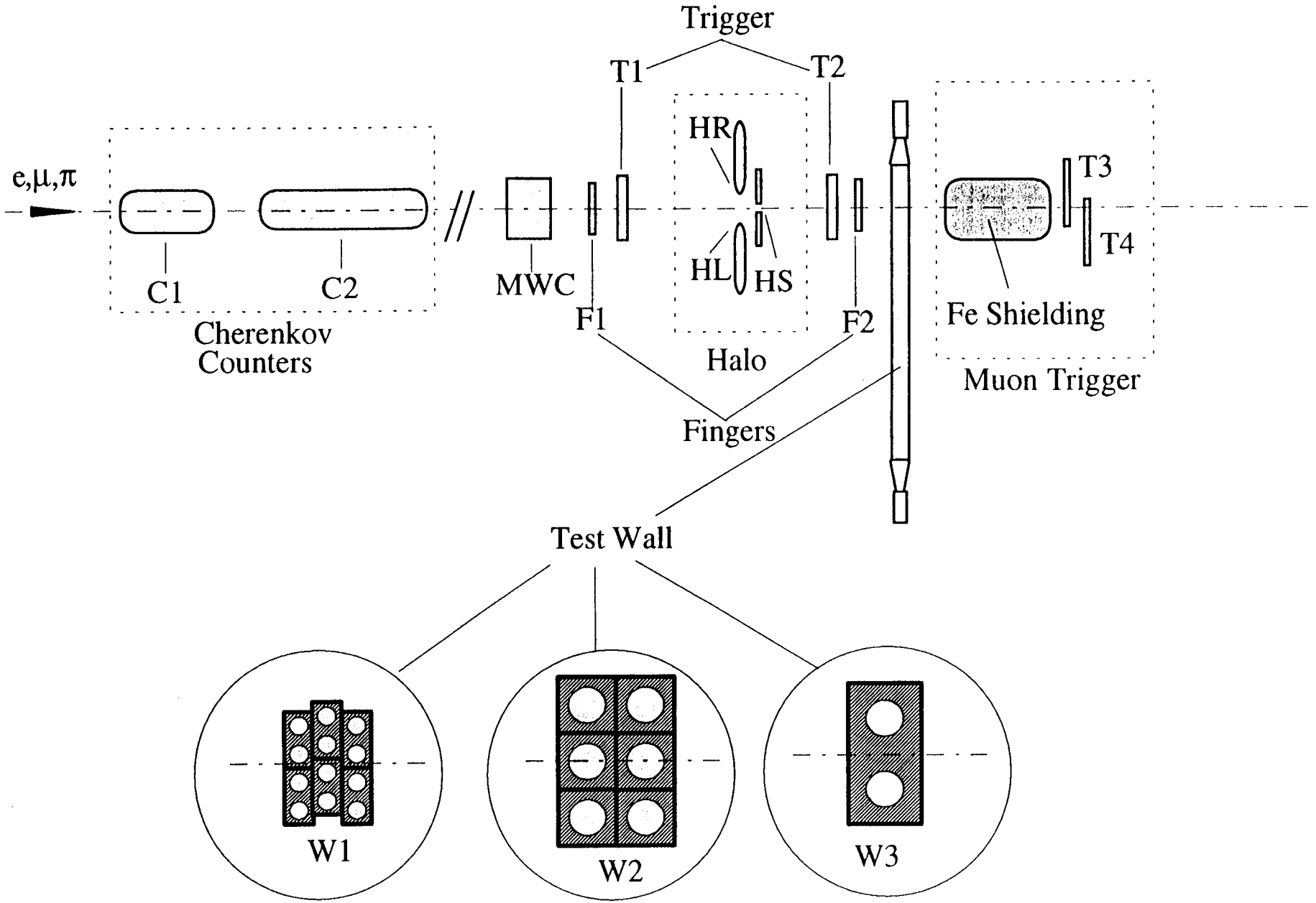
Trigger
T1
T2
HR
HL
HS
e,μ,π
C1
C2
Cherenkov
Counters
MWC
F1
F2
Halo
Fingers
T3
T4
Fe Shielding
Muon Trigger
Test Wall
W1
W2
W3

Fig. 7

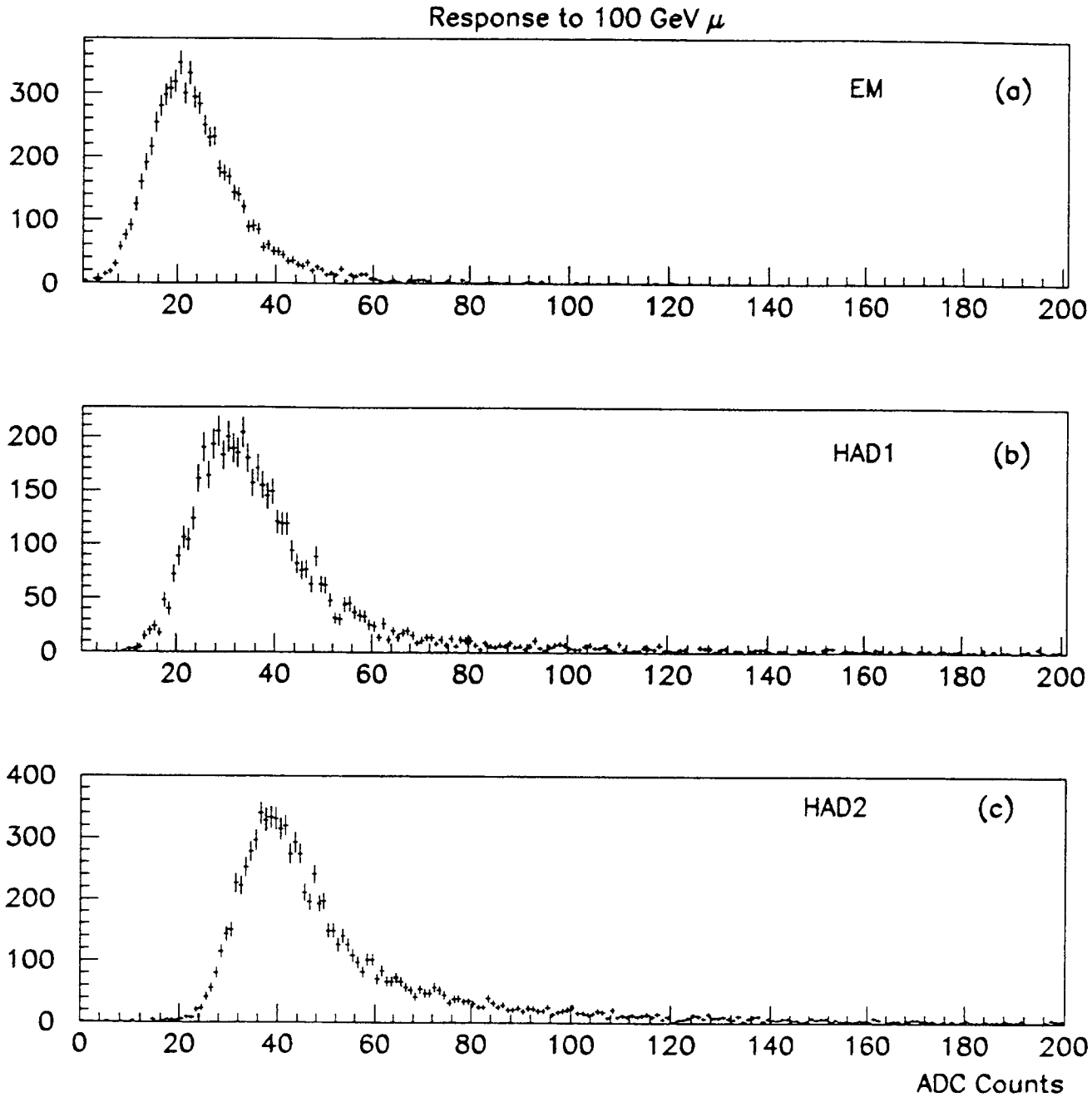

Fig. 8

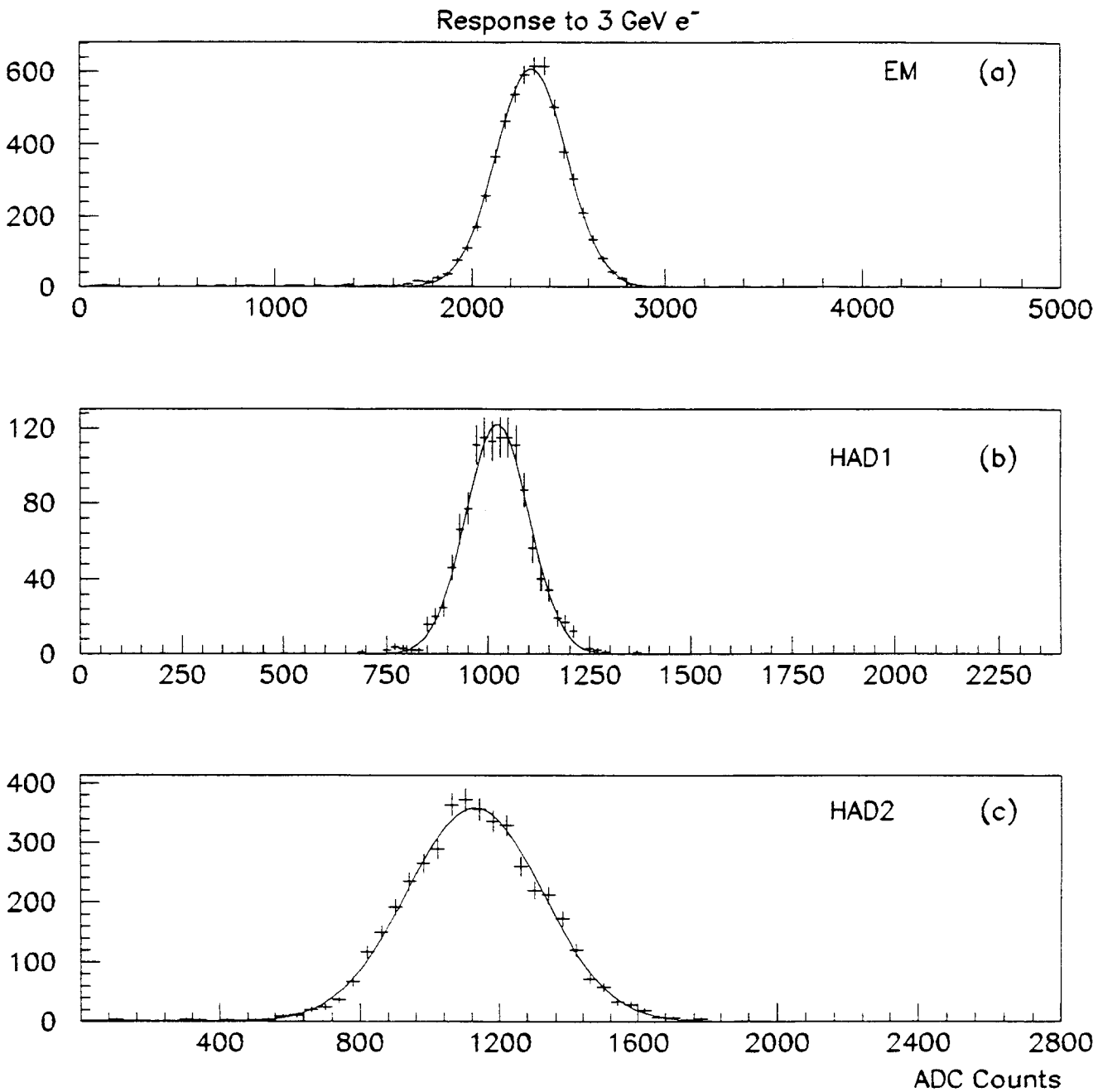
Response to 3 GeV e⁻
EM
(a)
600
400
200
0
0
1000
2000
3000
4000
5000
HAD1
(b)
120
80
40
0
0
250
500
750
1000
1250
1500
1750
2000
2250
HAD2
(c)
400
300
200
100
0
400
800
1200
1600
2000
2400
2800
ADC Counts

Fig. 9

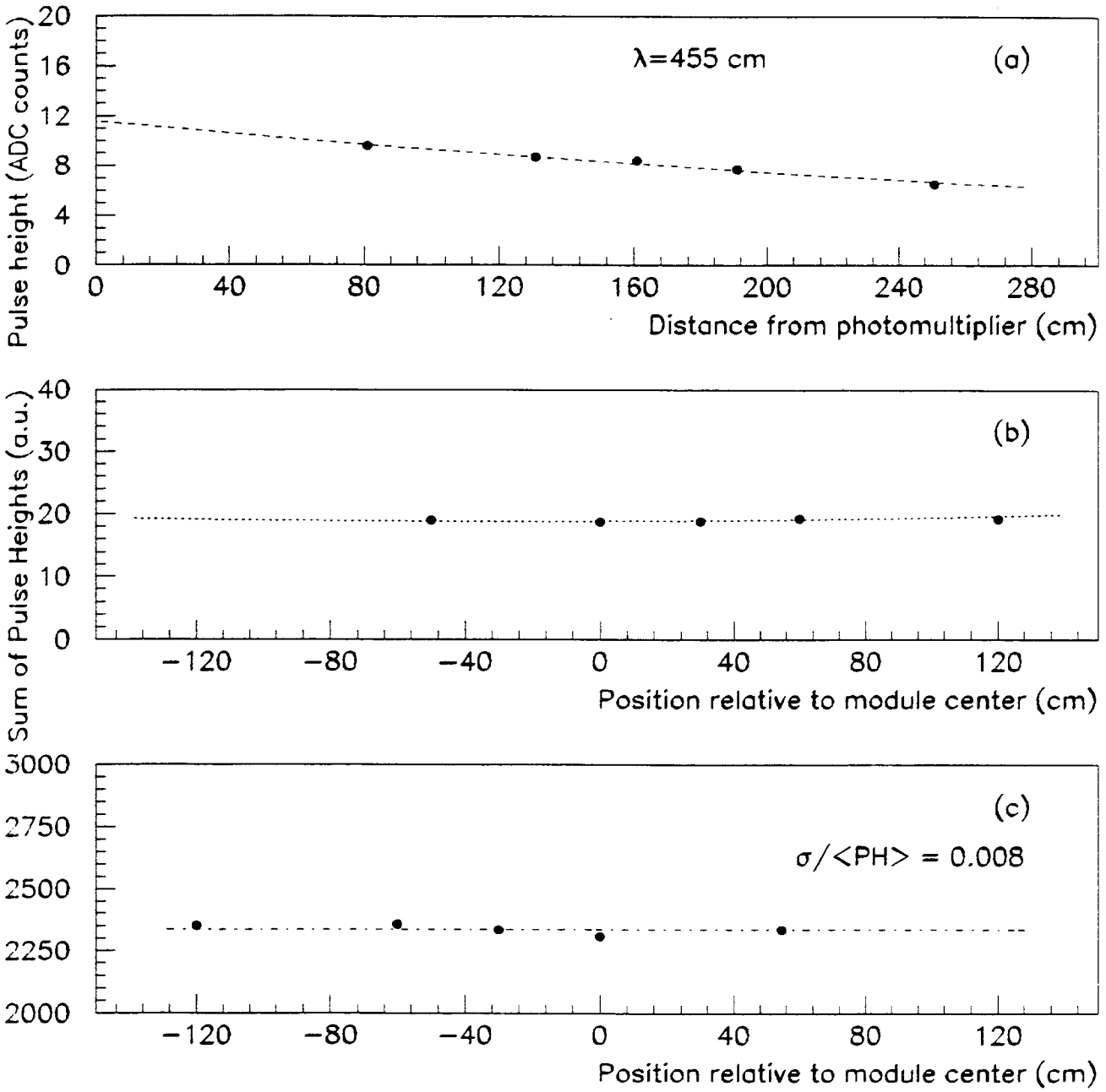
Pulse height (ADC counts)
20
16
12
8
4
0
λ=455 cm
(a)
0
40
80
120
160
200
240
280
Distance from photomultiplier (cm)
Sum of Pulse Heights (a.u.)
40
30
20
10
0
(b)
−120
−80
−40
0
40
80
120
Position relative to module center (cm)
3000
2750
2500
2250
2000
(c)
σ/<PH> = 0.008
−120
−80
−40
0
40
80
120
Position relative to module center (cm)

Fig. 10

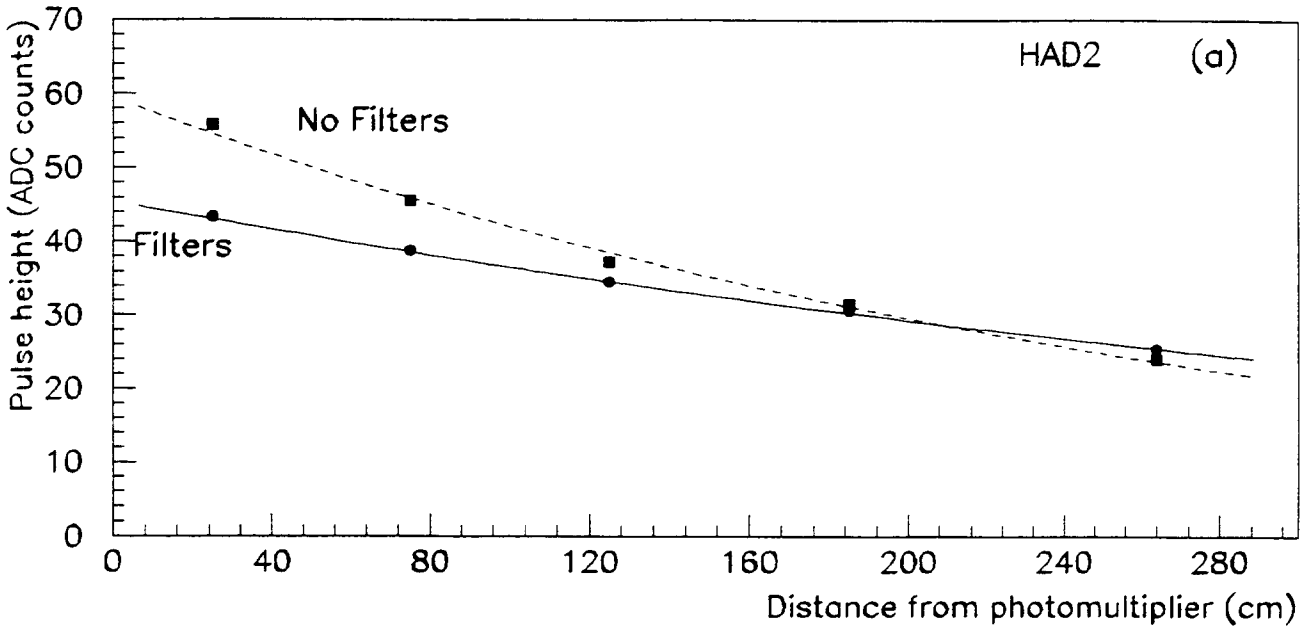
HAD2
(a)
No Filters
Filters
Pulse height (ADC counts)
70
60
50
40
30
20
10
0
0
40
80
120
160
200
240
280
Distance from photomultiplier (cm)

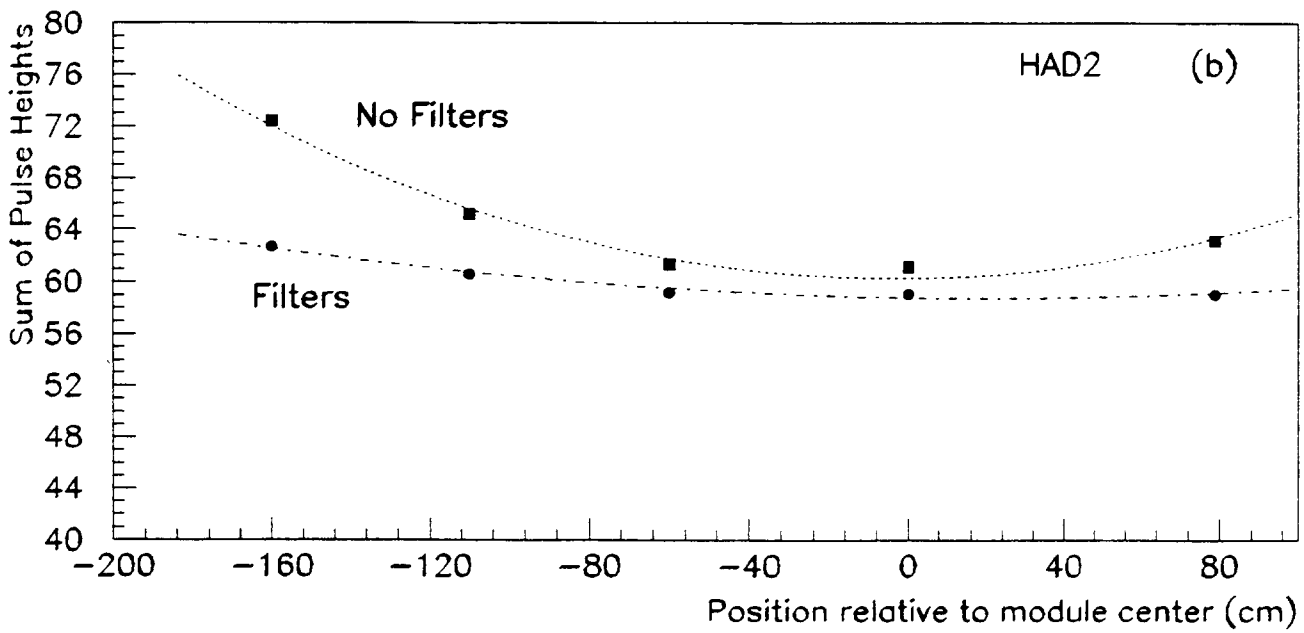
HAD2
(b)
No Filters
Filters
Sum of Pulse Heights
80
76
72
68
64
60
56
52
48
44
40
−200
−160
−120
−80
−40
0
40
80
Position relative to module center (cm)

Fig. 11

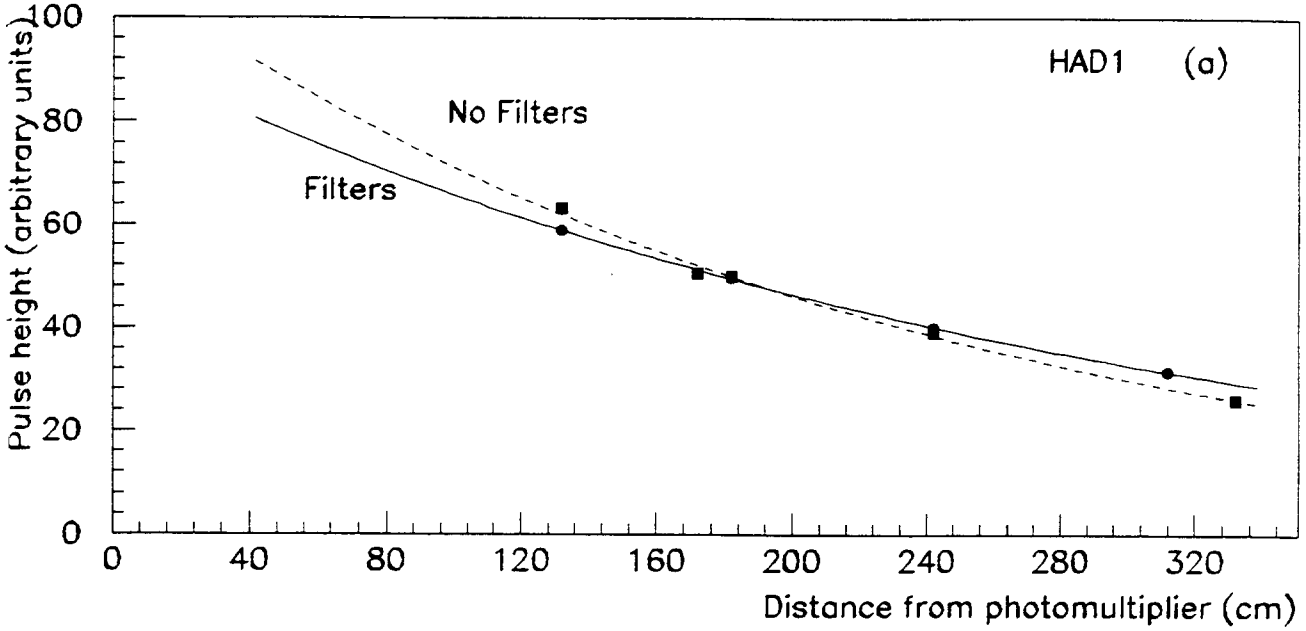
HAD1 (a)
No Filters
Filters
Pulse height (arbitrary units)
100
80
60
40
20
0
0
40
80
120
160
200
240
280
320
Distance from photomultiplier (cm)

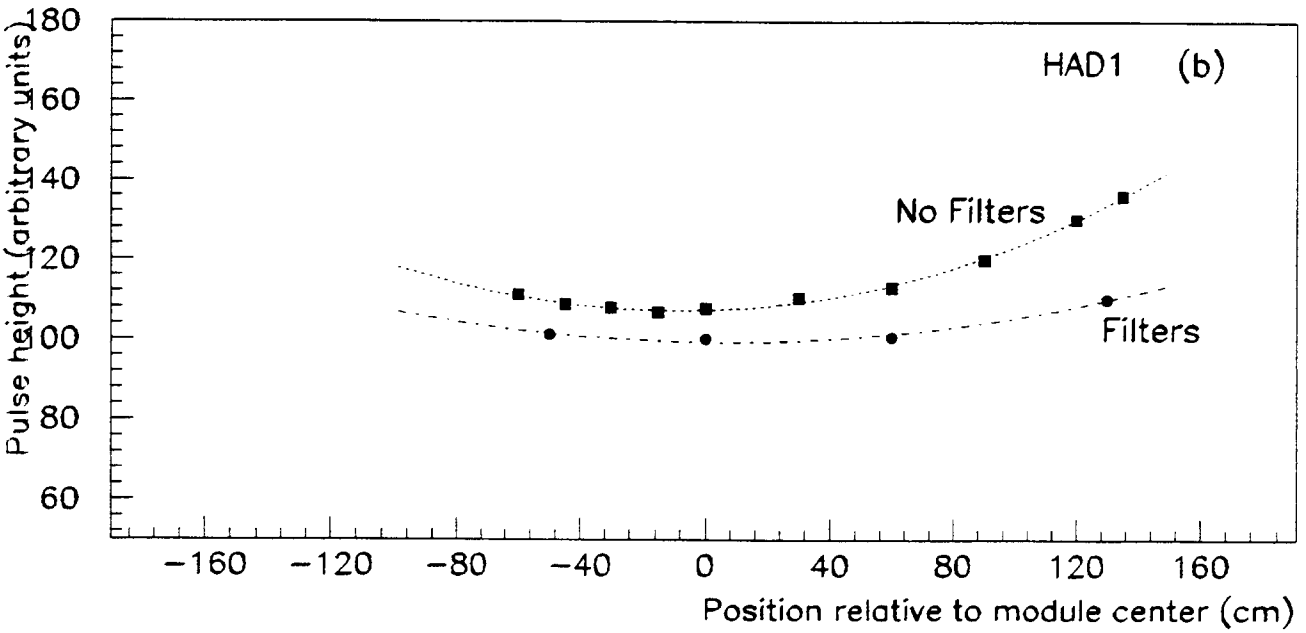
HAD1 (b)
No Filters
Filters
Pulse height (arbitrary units)
180
160
140
120
100
80
60
−160
−120
−80
−40
0
40
80
120
160
Position relative to module center (cm)

Fig. 12

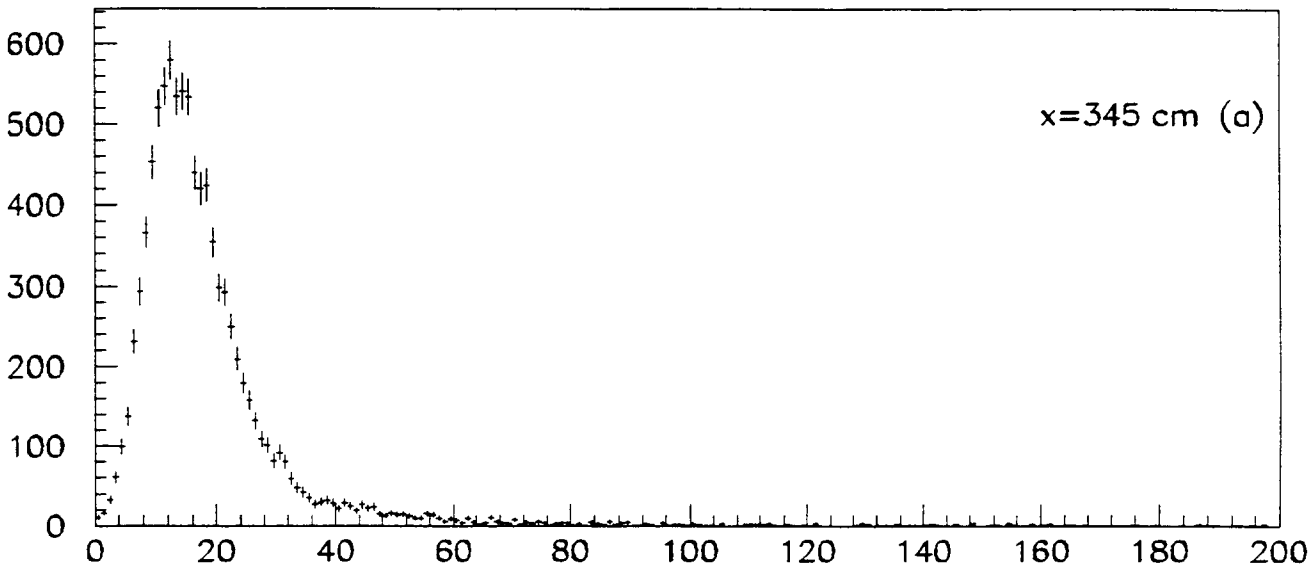
600
500
400
300
200
100
0
0
20
40
60
80
100
120
140
160
180
200
x=345 cm (a)

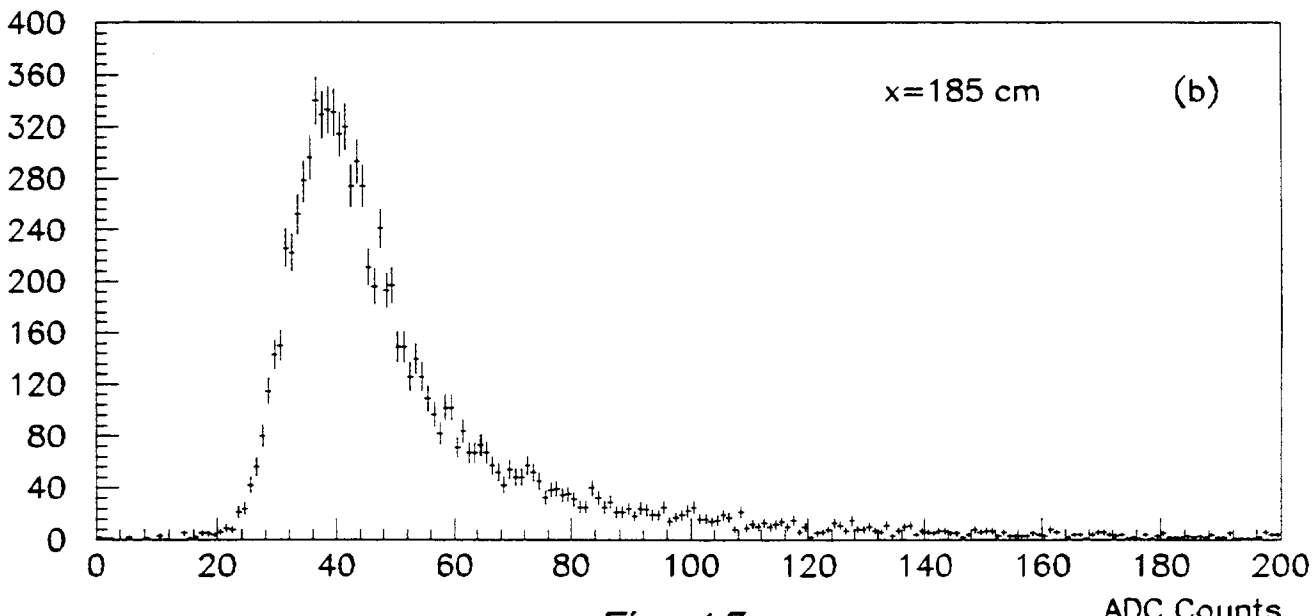
400
360
320
280
240
200
160
120
80
40
0
0
20
40
60
80
100
120
140
160
180
200
x=185 cm
(b)
ADC Counts

Fig. 13

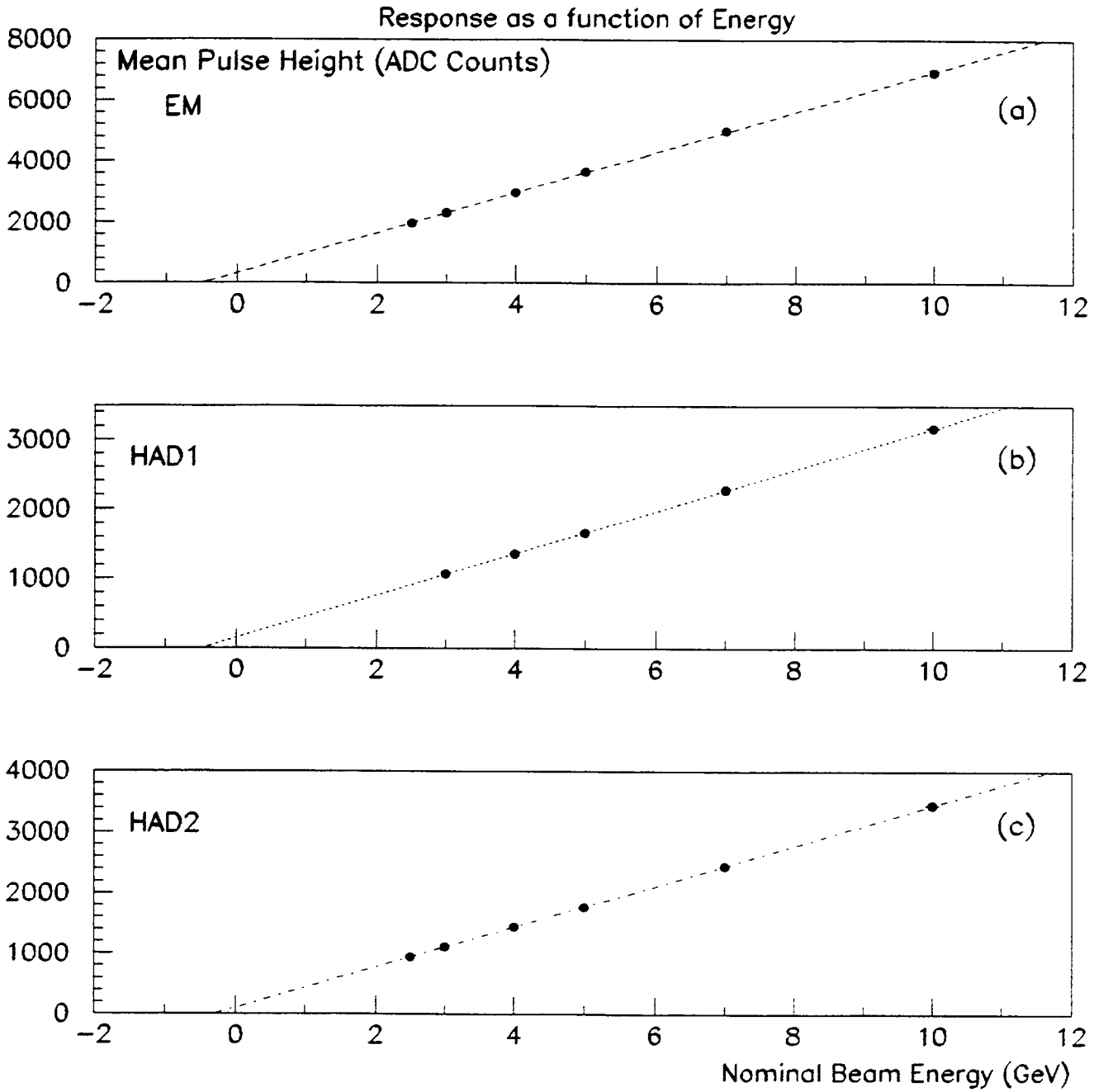
Response as a function of Energy
Mean Pulse Height (ADC Counts)
EM
(a)
8000
6000
4000
2000
0
−2
0
2
4
6
8
10
12
HAD1
(b)
3000
2000
1000
0
HAD2
(c)
Nominal Beam Energy (GeV)

Fig. 14

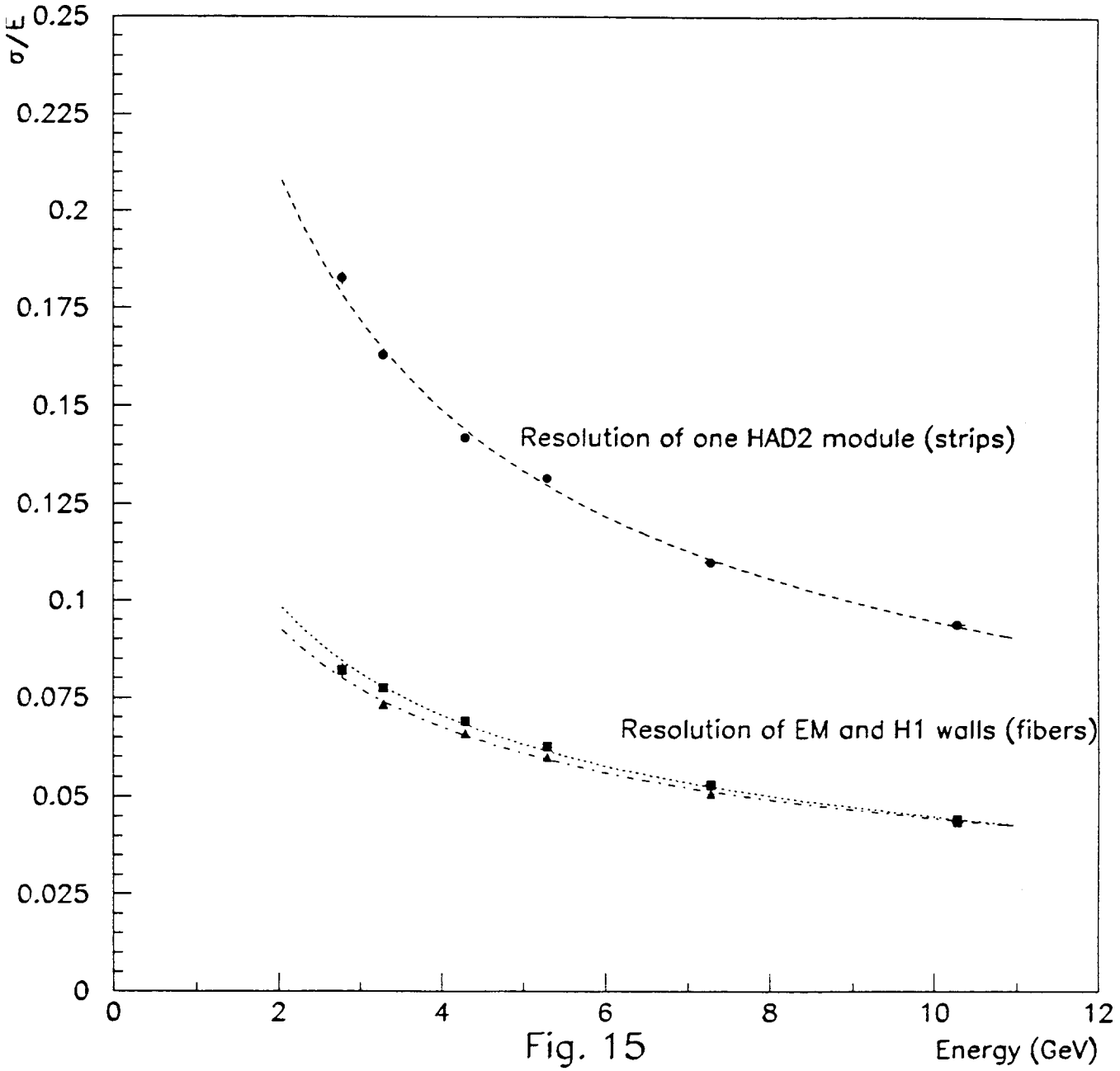
σ/E
0.25
0.225
0.2
0.175
0.15
0.125
0.1
0.075
0.05
0.025
0
0
2
4
6
8
10
12
Energy (GeV)
Resolution of one HAD2 module (strips)
Resolution of EM and H1 walls (fibers)

Fig. 15